Multiple-harmonic generation in rare gases at high laser intensity

X. F. Li, A. L'Huillier, M. Ferray, L. A. Lompré, and G. Mainfray
Service de Physique des Atomes et des Surfaces, Centre d'Etudes Nucléaires de Saclay, 91191 Gif-sur-Yvette, France

(Received 26 September 1988; revised manuscript received 3 January 1989)

We present experimental measurements of vacuum ultraviolet light emission processes in a 15-Torr rare-gas medium exposed to a strong 1064-nm laser field. Apart from a small number of lines which correspond to discrete transitions, and a broad continuum emission, we essentially observe the odd harmonics of the laser field, up to very high order. At a 3×10^{13} W cm^{-2} laser intensity, the highest-order harmonics observed are the 33rd in Ar, the 29th in Kr, and the 21st in Xe. The harmonic distribution presents three regions: a steep decrease for the first harmonics, a plateau, and a sudden cutoff at high order. We study the variation of the conversion efficiency for some of the harmonics as a function of the incident laser intensity and the atomic density. Finally, we analyze the harmonic-generation results as thoroughly as possible, in particular, by characterizing the phase-matching conditions in our experiment.

I. INTRODUCTION

An atom exposed to a strong laser field can absorb a large number of photons through high-order nonlinear processes. This leads to multiphoton ionization, above-threshold ionization (ATI), and multiple multiphoton ionization.[1] The energy absorbed by the atomic system may also be transferred back to the photon field under the form of energetic photons with energy $Nh\nu$, $h\nu$ being the laser photon energy and N the number of photons absorbed. Provided the medium has the required pressure and geometrical properties for proper phase matching of the generated radiation, one may expect production of high-order harmonics of the laser field.[2,3]

With the exception of two experiments using 1.06 (Ref. 4) and 1.315-μm (Ref. 5) laser radiation, most of the previous experiments[6–8] on harmonic generation in a gaseous medium use short incident wavelengths in order to obtain the shortest generated wavelengths. A number of experiments have been performed by using the fourth harmonic (266 nm)[6] of a Nd-YAG laser (where YAG is yttrium aluminum garnet) or the fundamental of an excimer laser, 308 nm (XeCl)[7] or 248 nm (KrF).[3,8] McPherson *et al.*[3] have recently reported up to the 17th harmonic in Ne using a 248-nm excimer laser at an intensity of 10^{16} W cm^{-2}. The conversion seems to be strongly dependent on the medium, since the highest-order harmonics reported in the same conditions in He, Ar, Kr, and Xe are, respectively, the 13th, the 7th, the 7th, and the 9th. Several authors[7,9–11] have also studied the dependence of high-order harmonic generation with the laser pump power and the gas pressure.

In this paper, we describe experimental measurements of vuv (vacuum ultraviolet) light emission (350–30 nm) and, in particular, harmonic generation in a rare-gas medium irradiated by a 1064-nm intense laser field. In a 10^{13}–W cm^{-2} intensity range, in a 15-Torr Ar gas jet, we observe the *odd* harmonics of the laser field, from the 3rd up to the 33rd harmonic. These results, reported previously by Ferray *et al.*,[2] are here described in more detail. We also study the variation of the conversion rate for some of the harmonics as a function of the atomic density and the laser intensity. Finally, we discuss the results in detail by examining the phase-matching conditions for these processes. Our aim is to disentangle the macroscopic effects (phase matching, absorption) and the microscopic effects, reflecting the response of each atom to the radiation field. Besides the harmonics, we also observe, in the same wavelength range a small number of lines corresponding to discrete transitions from excited states to the ground state and, especially in Xe, a broad continuum emission over the whole energy range investigated.

In Sec. II, we describe the experimental setup for detecting light emission over a very large spectral range. In Sec. III, we give a theoretical introduction to the problem of high-order harmonic generation and we introduce the main concepts and equations useful for the interpretation of the experimental results. These results are presented and discussed in detail in Sec. IV. We conclude in Sec. V.

II. EXPERIMENTAL ARRANGEMENT

The experimental arrangement, schematized in Fig. 1, consists of three parts: the laser, the pulsed gas jet, and the detection system. We use the fundamental frequency (1064 nm) of a mode-locked Nd-YAG laser. The 36-psec-length bandwidth limited pulse is amplified up to a 1-GW power at a 10-Hz repetition rate. The energy is varied after amplification by rotating a half-wave plate placed before a polarizer and measured by a calorimeter. The linearly polarized beam is focused by a 200-mm focal length lens. The intensity is determined by reference to ion detection measurements performed previously[12] in the following way: Using the same apparatus shown in Fig. 1, we introduce a gas at low pressure (10^{-5} Torr) and we measure the ions produced during the interaction

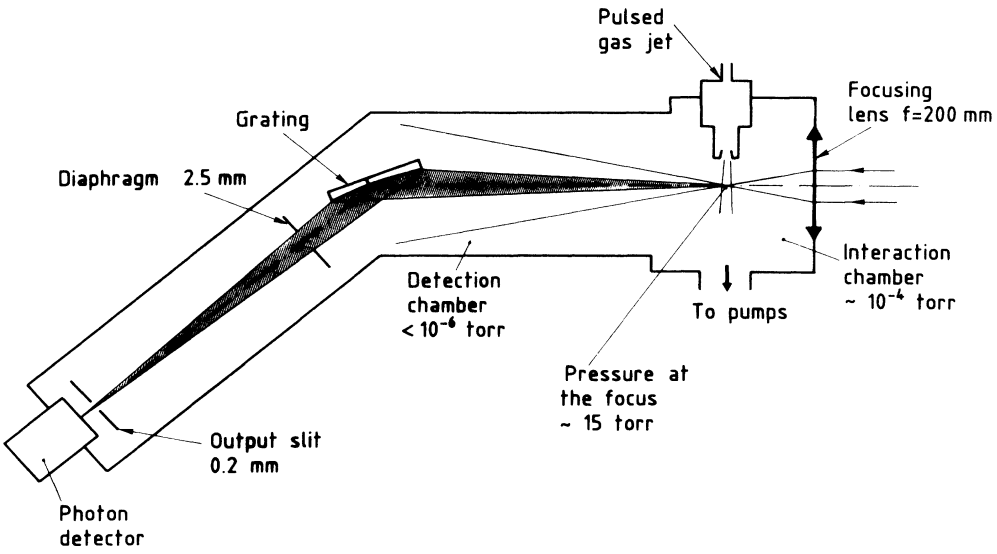

FIG. 1. Experimental setup for the detection of vuv light.

using a time-of-flight spectrometer. The saturation intensity, at which the ionization probability becomes equal to unity, is determined by studying the laser intensity dependence of the number of singly charged ions. The saturation intensities for the rare gases, indicated in Table I have been determined previously.[12] We can then calibrate our laser system by reference to these data. The beam radius at the focus, deduced from this calibration, is $R=18$ μm. Assuming a Gaussian spatial distribution, the laser confocal parameter is $b=4\pi R^2/\lambda=4.2$ mm, with $\lambda=1064$ nm.

The gas jet used in the present experiment has been described in detail elsewhere[13] and we shall only recall its main characteristics. It is an injector-type of device, with an electromagnetically actuated valve. The opening time of the valve is 250 μsec. The backup pressure remains low, 150 Torr, which minimizes the formation of dimers. The interaction chamber is pumped down by a 800-l/s turbomolecular pump at a background pressure of 5×10^{-9} Torr and at pressure of 2×10^{-4} Torr when the gas jet is operating at 10 Hz. The pressure in the detection chamber, pumped down by an additional oil diffusion pump, remains lower than 10^{-6} Torr, which limits the reabsorption of the vuv light on its way to the analyzer.

The gas-jet characteristics (density, profile) are determined by measuring the laser-induced fluorescence light emitted perpendicularly to the laser axis. We study the fluorescence signal as a function of the distance nozzle focus and we compare it to the signal measured in a cell, with the same experimental conditions, at various static pressures (see Ref. 13 for more details). Our 6-mm-nozzle-length gas jet is well collimated. The pressure can be varied from 0.3 Torr at 4 mm from the nozzle up to 25 Torr at 0.1 mm. Most of the results presented in this paper have been obtained at 15 Torr (0.5 mm from the nozzle, 1 mm beam diameter).

The vuv light is analyzed along the laser axis by using a grating monochromator. As shown in Fig. 1, the focus plays the role of the entrance slit of the monochromator in order to have the best collection efficiency. A 2.5 mm wide slit is added after the grating to protect the detector from the scattered light induced by the infrared laser light. The vuv light is analyzed with a Pt-coated toroidal holographic grating at grazing incidence. We use two gratings, the first one from 50 to 350 nm, with 275 lines/mm, 8 Å resolution, blazed at 100 nm; the second one from 10 to 50 nm, with 550 lines/mm, 4 Å resolution, blazed at 15 nm. The spectral efficiencies of these gratings are extracted from experimental measurements performed by the manufacturer (Jobin-Yvon).

Finally, the vuv light is detected by photomultipliers (an XP 2020Q RTC from 200 to 350 nm and a solar blind EMI GENCOM from 100 to 200 nm) or a windowless electron multiplier (16F RTC) at wavelengths below 120 nm. The spectral efficiencies of these detectors are estimated by using response curves given by the manufacturers, and at short wavelengths by using the

TABLE I. Saturation intensities for the rare gases (Ref. 12). The experimental uncertainty is ±50%. $x[y]=x\times10^{y}$.

	Xe	Kr	Ar	Ne	He
I_s (W cm^{-2})	1.2[13]	2.5[13]	3[13]	1.9[14]	2.8[14]

photoelectric yield of CuBe (of which the dynodes of our electron multiplier are made) given by Samson.[14]

Finally, we estimate that the experimental uncertainty for the relative measurements of the uv intensity at different frequencies is of the order of a factor of 5. This important uncertainty arises from the use of several devices (gratings and detectors), of which the spectral response is not always accurately known and which are needed in order to cover a broad spectral range.

III. THEORETICAL BACKGROUND

The interaction of an ensemble of atoms with an intense laser field may lead to several vuv light emission processes. In our experimental conditions, below the breakdown threshold, one may expect to observe, among other possible processes, (i) *fluorescence* from states excited through multiphoton absorption (for example, $A+Nh\nu\rightarrow A^{+*}+e$; $A^{+*}\rightarrow A^{+}+h\nu_{uv}$); (ii) *harmonic generation* ($A+Nh\nu\rightarrow A+h\nu_{uv}$); (iii) *fluorescence* from states excited through recombination processes (for example, $A^{+}+e\rightarrow A^{*}\rightarrow A+h\nu_{uv}$).

In our experiment, at 10^{13} W cm^{-2}, it turns out that there is no clear evidence for process (i). A small number of lines may be attributed to process (iii). The most important vuv emission process observed is the production of high-order harmonics of the laser field, up to the 33rd in Ar. In the present paper, we concentrate on these harmonic conversion results. Before reporting these results, we recall the main equations which govern harmonic generation in a gaseous medium.[15,16]

The propagation equation relating the qth harmonic field E_q to the nonlinear polarization of the medium P_q^{NL} can be written as

$$\nabla_{\perp}^2 E_q+2ik_q\frac{\partial}{\partial z}E_q=-\frac{4\pi}{c^2}(q\omega)^2P_q^{\mathrm{NL}}e^{-i\Delta k_q z}, \tag{1}$$

where $\nabla_{\perp}$ acts on the transverse coordinate $\mathbf{r}$, ω is the incident laser frequency, k_q is the wave vector of the qth harmonic field, c is the speed of light, and Δk_q is the phase mismatch between E_q and P_q^{NL}. In order to complete the description of the nonlinear optical interaction, one must specify the dependence of the polarization on the (incident and generated) optical fields.

High-order harmonic generation may be accomplished through a *direct* process (absorption of q laser photons, emission of one photon at frequency $q\omega$) and also through *indirect* processes, in which harmonic generation is due to a lower-order wave-mixing process involving the fundamental and lower-order harmonic fields.[4,7,17] In our experimental conditions, the mechanism responsible for harmonic generation is more probably the direct process, because of the intense incident field and the low harmonic-conversion efficiency. Neglecting indirect processes, the *lowest-order* contribution to the nonlinear polarization oscillating at frequency $q\omega$ is related to the laser field E_1 by

$$P_q^{\mathrm{NL}}(\mathbf{r},z,t)=\frac{1}{2^{q-1}}\mathcal{N}\chi^{(q)}(-q\omega;\omega,\omega,\ldots,\omega)E_1^q, \tag{2}$$

where $\chi^{(q)}$ denotes the qth order nonlinear susceptibility and $\mathcal{N}$ the atomic density. Equation (1) for $q>1$, becomes

$$\nabla_{\perp}^2 E_q+2ik_q\frac{\partial}{\partial z}E_q=-\frac{4\pi}{c^2}(q\omega)^2\frac{\mathcal{N}\chi^{(q)}}{2^{q-1}}E_1^q e^{-i\Delta k_q z}, \tag{3}$$

with $\Delta k_q=k_q-qk_1$.

Let us now consider the case of an incident Gaussian beam focused into a nonlinear medium of finite length:

$$E_1(\mathbf{r},z,t)=\frac{E_{10}}{1+2iz/b}e^{-k_1r^2/b(1+2iz/b)}e^{-\alpha t^2/\tau^2}, \tag{4}$$

where b is the laser confocal parameter, E_{10} is the maximum amplitude of the field, $z=0$ corresponds to the position of the focus, $\alpha=1.38$ ($2\ln 2$), and τ is the laser pulse duration. Equation (4) can then be analytically solved.[18–21] The qth harmonic field generated in a uniform medium extending from $-L/2$ to $L/2$ has also a Gaussian profile with the same confocal parameter and beam-waist location as the fundamental field. Its amplitude is given by

$$E_q(\mathbf{r},z,t)=-\frac{iq\pi^2b\mathcal{N}\chi^{(q)}}{n_q2^{q-2}\lambda}\frac{E_{10}^q}{1+2iz/b}\times e^{-qk_1r^2/b(1+2iz/b)}\times e^{-\alpha qt^2/\tau^2}F_q(b\Delta k_q), \tag{5}$$

where n_q is the refractive index at $q\omega$. The phase-matching optimization integral $F_q(b\Delta k_q)$ is defined by

$$F_q(b\Delta k_q)=\int_{-L/2}^{L/2}(1+2iz/b)^{1-q}e^{-iz\Delta k_q}2dz/b. \tag{6}$$

The qth harmonic-field maximum intensity (I_q) is related to the incident laser field maximum intensity I by

$$I_q=\frac{2^{q+1}b^2q^2\pi^{q+3}}{n_1n_q\lambda^2c^{q-1}}I^q|F_q|^2|\mathcal{N}\chi^{(q)}|^2. \tag{7}$$

Equation (7) involves two important terms, the qth order (atomic) susceptibility $\chi^{(q)}$, which characterizes the response of each individual atom to the radiation field, and the phase-matching factor F_q, which describes the response of the whole medium (and which depends on macroscopic quantities such as geometry, pressure, or dispersion). The conversion efficiency is influenced by both the atomic and the collective response of the gaseous medium, which makes the interpretation of the experimental results rather difficult. It is therefore important to examine, when possible, the respective contributions of the nonlinear susceptibilities and the phase-matching conditions to the production of the harmonics of the laser field.

Let us examine the phase-matching conditions in our experiment. Figure 2 shows $|F_q|^2$ for q odd varying from 3 to 33, as a function of the dimensionless parameter $b\Delta k$ calculated for our experimental conditions. Figure 2(a) refers to a 1-mm-long uniform medium (extending from $-L/2$ to $L/2$ with $L=1$ mm). In Fig. 2(b), we have modeled our gas jet in a more realistic way, by using a Lorentzian distribution with a 1 mm width at half max-

TABLE II. Optical parameters for the rare gases. The phase mismatches are deduced from Ref. 22. The susceptibilities $\chi_0^{(3)}$ are experimental values from Ref. 29 (given at ±10%); we have multiplied the values given in Ref. 29 by a factor of 4, to be consistent with our definition of the nonlinear susceptibilities. The susceptibilities $\chi^{(q)}$ are extracted from the experimental results and normalized to $\chi_0^{(3)}$ in Xe. They are given within ±50%. $x[y]=x\times 10^{y}$.

	Xe	Kr	Ar	Ne	He
Δk_3 (cm^{-1})	2.[−1]	9.2[−2]	4[−2]	2.8[−3]	1.9[−3]
Δk_5 (cm^{-1})	1.1	4.5[−1]	1.9[−1]	1.6[−2]	9.2[−3]
$\chi_0^{(3)}$ (esu)	6.9[−37]	2.3[−37]	8.6[−38]	6.5[−39]	3.6[−39]
$\chi^{(3)}$ (esu)	6.9[−37]	2.3[−37]	9.2[−38]	4.6[−39]	2.3[−39]
$\chi^{(5)}$ (esu)	8[−48]	1.4[−49]	2.1[−50]	4.6[−51]	

imum for representing the nonuniform atomic density in the jet.[21]

Equation (6) is replaced by

$$F_q(b\Delta k)=\int_{-\infty}^{+\infty}(1+2iz/b)^{1-q}\times\exp[-iL\Delta k\arctan(2z/L)/2]\times 2dz/b(1+4z^2/L^2)\,. \quad (8)$$

Our experimental setup is such that the radiation beam remains approximately collimated throughout the medium ($b=4.2$ mm $>$ $L=1$ mm). A rough approximation to Eq. (6) or Eq. (8) in this particular case, which helps in understanding the results shown in Fig. 2, consists in taking the limit $b\gg L$. $|F_q|^2$ then takes the simple form

$$|F_q|^2=(2L/b)^2\left[\frac{\sin(\Delta k_{\text{eff}}L/2)}{\Delta k_{\text{eff}}L/2}\right]^2. \quad (9)$$

Equation (9) is similar to the expression for a plane wave, except that Δk_q is replaced by $\Delta k_{\text{eff}}=\Delta k_q+2(q-1)/b$, representing an effective phase mismatch[15,20] between the qth harmonic wave and the polarization at $q\omega$. Δk_{eff} is the sum of two terms; Δk_q, a phase mismatch originating from the difference in the dispersive properties of the medium at ω and $q\omega$; and $2(q-1)/b$, a *geometrical* phase mismatch originating from the phase shift undergone by a Gaussian beam across the focus. This latter term is responsible for the q-dependent shift of the maximum of the phase-matching integrals, centered at $b\Delta k_{\text{eff}}=0$ [$b\Delta k=-2(q-1)$] (see Fig. 2).

To complete this discussion of the phase-matching conditions in our experiment, we must estimate the phase mismatch $\Delta k_q=k_q-qk_1=(n_q-n_1)\,q\omega/c$. Let us distinguish three energy regions.

(i) $q\omega$ below the first excited state. Δk is positive and small. The linear refractive indices for the rare gases do not vary much before the first excited states and moreover, the atomic density in the gas jet is rather low. Table II shows the values of Δk_3 and Δk_5 for the rare gases at 15 Torr ($\mathcal{N}=5\times 10^{17}$ atoms/cm^3) and 1.064 μm, deduced from experimentally measured refractive indices.[22] The parameter $b\Delta k$ remains very small compared to the widths of the phase-matching integrals (Fig.2). Our medium can be considered *dispersionless* in this energy region.

(ii) $q\omega$ in the region of the discrete excited states. Δk follows the variation of the refractive index at $q\omega$, which may become very large (or very small) in the vicinity of resonances. This may lead to the breaking of phase-matching conditions and also reabsorption of the generated light.

(iii) $q\omega$ above the ionization threshold. n_q (and therefore Δk) becomes imaginary. The imaginary part is responsible for the absorption of the generated radiation due to photoionization.[23–25] The real part of the phase

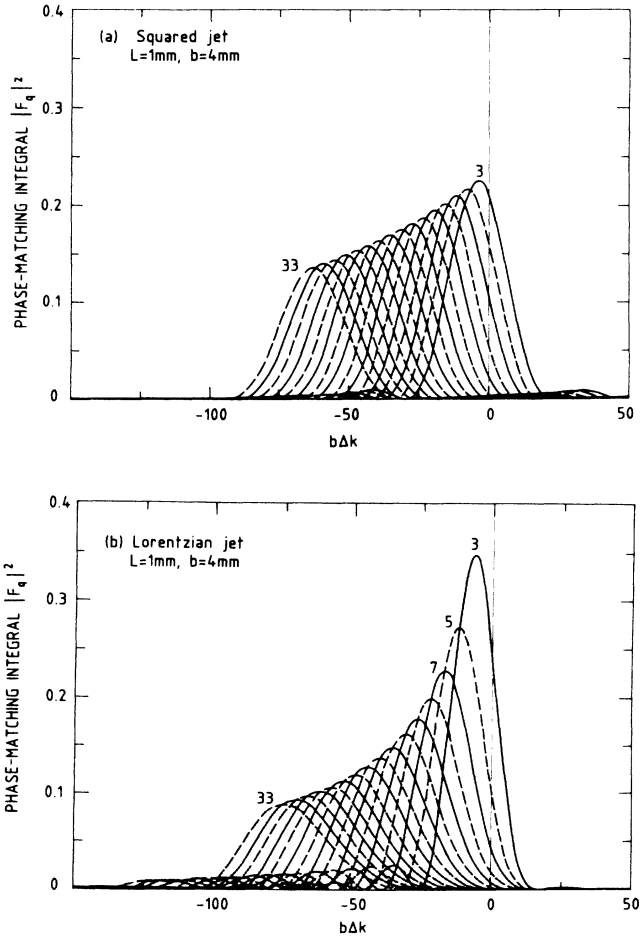

FIG. 2. Phase optimization integrals $|F_q|^2$ as a function of $b\Delta k$ for q odd = 3 to 33 and $b=4.2$ mm, with a uniform (a) and Lorentzian (b) atomic density with 1 mm width at half-maximum.

mismatch is negative, but it remains small compared to the widths of the phase-matching peak because of the low pressure.

In summary, apart possibly from particular frequencies corresponding to discrete excitations, we may perhaps consider the nonlinear medium in our experiment to be dispersionless. $\Delta k \approx 0$, so that $\Delta k_{\text{eff}} \approx 2(q-1)/b$. The phase-matching factor $|F_q|^2$ is close to optimal phase matching for the first harmonics, and decreases rapidly with q, as shown in Fig. 3 for the two cases studied (squared and Lorentzian gas jet). Very different situations could be obtained in other experimental conditions, e.g., in a cell ($L \gg b$).[26]

However, this discussion is of course only valid in a weak-field approximation. Other effects due to the ionization of the medium or due to the high intensity may change the atomic response (nonlinear susceptibilities) and also the phase-matching conditions. In the present work, we shall interpret and discuss our experimental results within this theoretical framework, being aware of its limitations. We shall also, when possible, point out the results which can be understood within lowest-order perturbation theory and with a proper description of the phase-matching conditions in our experiment and those which, on the contrary, indicate a departure from what can be expected from this weak-field theory.

IV. EXPERIMENTAL RESULTS

We first describe the harmonic-generation results. We shall briefly present other light emission processes also observed in our experiment in Sec. IV D.

A. Harmonic-intensity distributions

In Fig. 4, we plot the number of photons detected (in a logarithmic scale) for each harmonic of the laser field, in Ar, at 3×10^{13} W cm^{-2} and 15 Torr. The vertical scale is an estimation (within about one order of magnitude) of the number of harmonic photons produced at each laser shot. The error bar indicated in Fig. 4 refers to the *relative* measurements of the harmonics intensity. We only observe *odd* harmonics (we did not, however, look for second-order harmonic generation). This is to be expected for harmonic generation in an isotropic gaseous medium with inversion symmetry.

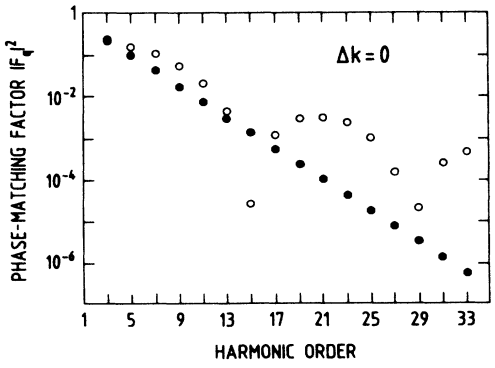

FIG. 3. Phase-matching factor $|F_q|^2$ evaluated at $\Delta k=0$; ○, squared jet; ●, Lorentzian jet.

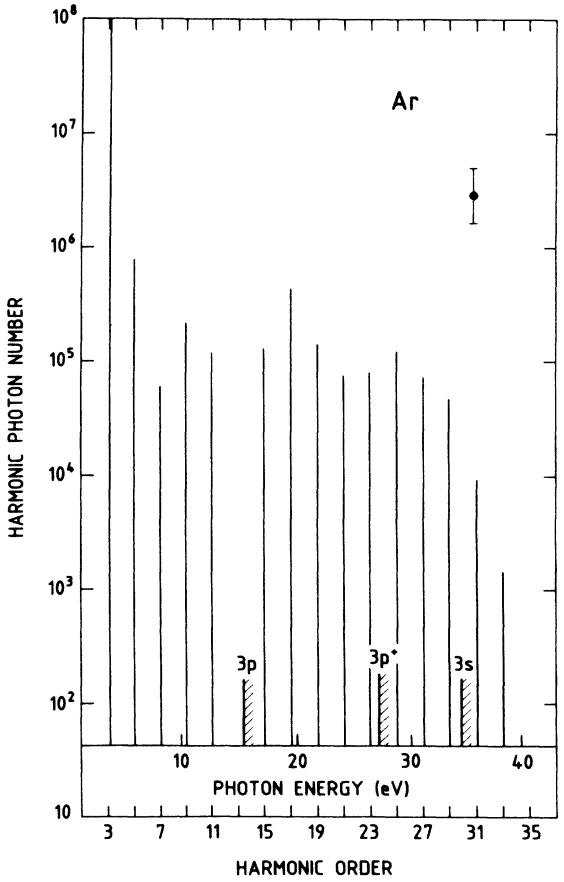

FIG. 4. Harmonic-intensity distribution in Ar at 3×10^{13} W cm^{-2} and a 15 Torr pressure.

The distribution presented in Fig. 4 decreases first rather steeply from the third to the seventh harmonic; it presents a kind of plateau from the 7th to the 27th with a missing 13th harmonic; finally, it decreases again rather steeply down to the 33rd harmonic. We have also indicated in Fig. 4 a photon energy scale in eV (the laser photon energy is 1.165 eV) and some characteristic ionization energies of Ar, namely, the $3p$ and $3s$ ionization energies and the $3p$ ionization energy of Ar^+ (denoted $3p^+$ in Fig. 4).

The energy of 13 laser photons is just below the ionization limit, in the region of discrete excited states (which may be strongly perturbed and shifted at the intensities used in our experiment). Let us propose two tentative explanations for the disappearance of the 13th harmonic. First, as discussed in Sec. III, it may be due to breaking of phase-matching conditions induced by the change of the refractive index in the vicinity of $J=1$ resonances and reabsorption of the vuv light by the atom at this particular frequency. Alternatively, multiphoton ionization may be enhanced compared to harmonic generation in the vicinity of resonances with $J\neq1$ states, not contributing to harmonic generation because of the electric dipole selection rules.

In Figs. 5 and 6, we present similar distributions obtained in Kr and Xe in the same experimental conditions, i.e., a laser intensity of 3×10^{13} W cm^{-2} (above the saturation intensity for ionization in both gases) and a 15 Torr pressure. The Xe distribution is similar to the Ar result (without any missing harmonic). In contrast, the distribution obtained in Kr looks more scattered.

In the same conditions (same pressure and intensity), the conversion efficiency for the first harmonics increases with Z (from Ar to Xe). For example, the numbers of photons in the region of the plateau are approximately equal to 10^5 in Ar, 10^6 in Kr, and 10^7 in Xe. On the other hand, the distributions, are more and more spread out from Xe to Ar. We detect up to the 21st harmonic in Xe, 29th harmonic in Kr and 33rd harmonic in Ar. Note the rather abrupt cutoff, especially in Xe (the number of 23rd-harmonic photons is lower than 10^3, at least three orders of magnitude less than for the 21st harmonic).

The position of the cutoff approximately corresponds to the ionization energy in the s atomic subshell ($3s$, $4s$, and $5s$ in Ar, Kr, and Xe, respectively). We do not see at present how ionization in the external s subshell could influence harmonic generation. This coincidence shows anyway that the position of the cutoff in the harmonic distribution closely follows the scaling laws of the rare gases. The cutoff may be related to the ionization of the medium (saturation), if we assume that harmonic generation in an ionized medium is much less probable that harmonic generation in a neutral medium.

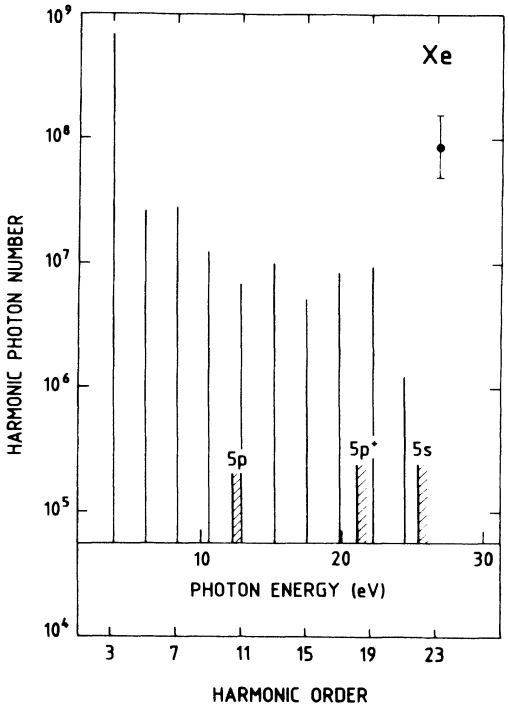

FIG. 6. Harmonic-intensity distribution in Xe at 3×10^{13} W cm^{-2}, 15 Torr.

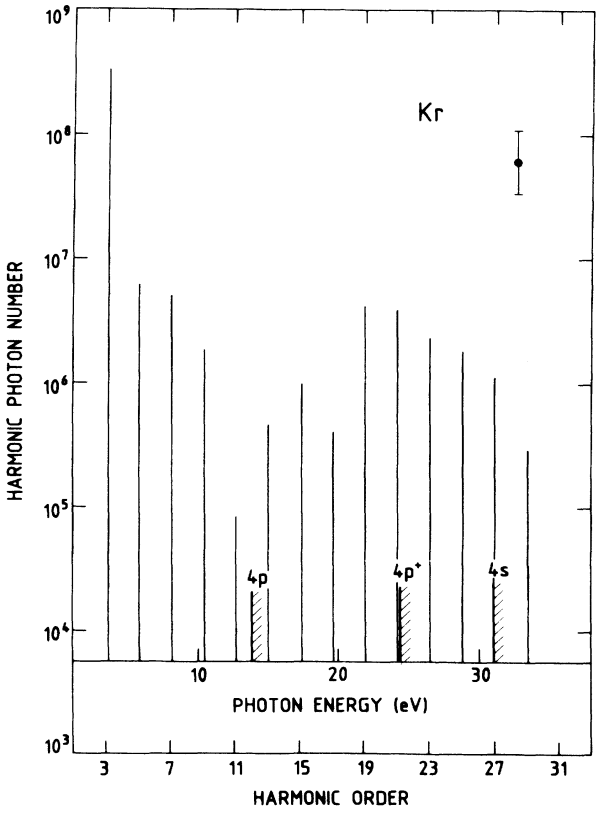

FIG. 5. Harmonic-intensity distribution in Kr at 3×10^{13} W cm^{-2}, 15 Torr.

The results shown in Figs. 4–6 are similar to the earlier measurements presented in Ref. 2, except for the ratio of the third to the fifth harmonic intensities. The measurement of this ratio has been improved in the present work by using a photomultiplier more adapted to the 200–350-nm wavelength range. Compared to the value given in Ref. 2, the new value for the ratio is reduced by about one order of magnitude.

Finally, although we observed extremely high-order harmonic generation in Xe, Kr, and Ar, in the same experimental conditions, namely, 15 Torr and 3×10^{13} W cm^{-2}, we did not get harmonics of higher order than the third in He and the fifth in Ne. As mentioned above, as Z decreases, the average harmonic-conversion efficiency for the first harmonics decreases, but higher-order harmonics can be generated (in simple words, the plateau goes down but extends further out). Extrapolating this conclusion to Ne and He, we think that we did not have a low enough detection threshold, or enough laser power, to see the plateaus in these two gases. We may expect, given enough laser intensity, to generate even higher-order harmonics in Ne and He.

In Fig. 7, we present harmonic-intensity distributions obtained in Ar, at a 15 Torr pressure, at three different intensities (a) 3×10^{13} W cm^{-2} (same result as in Fig. 4), (b) 2.2×10^{13} W cm^{-2}, (c) 1.6×10^{13} W cm^{-2}. The highest laser intensity is the saturation intensity for ionization of Ar, at which the multiphoton ionization proba-

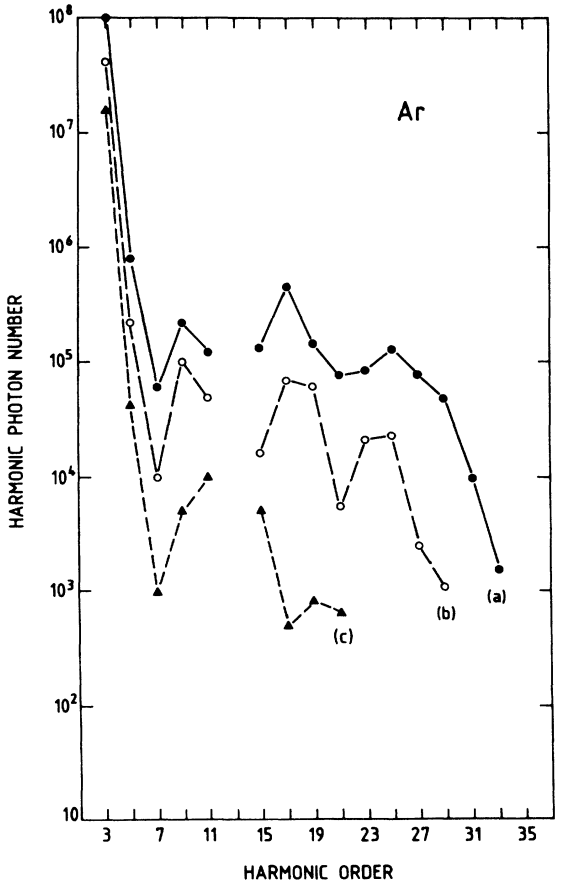

FIG. 7. Harmonic-intensity distribution in Ar at 15 Torr and several laser intensities (a) 3×10^{13} W cm^{-2}, (b) 2.2×10^{13} W cm^{-2}, (c) 1.6×10^{13} W cm^{-2}.

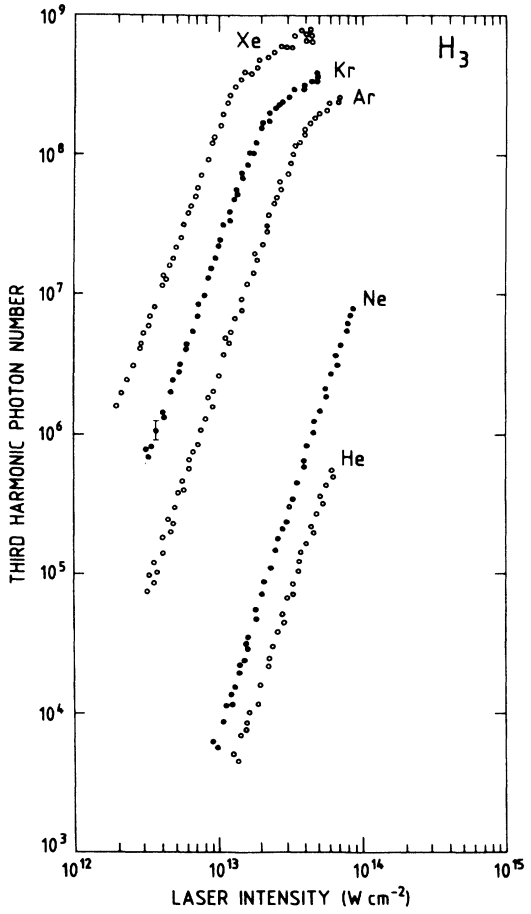

FIG. 8. Laser-intensity dependence of the number of photons at the third harmonic in Xe, Kr, Ar, Ne, and He, at a 15 Torr pressure.

bility becomes equal to unity. Of course, this is a low-pressure result and one may ask whether it can be extrapolated at a 15 Torr pressure. Harmonic generation is a fast process, which does not last longer than the laser pulse. Collisional processes which may change the value of the intensity at which the interaction volume becomes ionized, and which are eventually responsible for the plasma thermalization, probably take place over a longer time period. We shall assume that, during the 36-psec pulse duration, the dominant ionization mechanism is multiphoton ionization. The ionization rates corresponding to the intensities in Fig. 7 are then approximately 1, 10^{-2}, and 10^{-4}. Most of the harmonics are created at an intensity such that the medium is not or weakly ionized. This seems to rule out plasma effects[27,28] as responsible for the production of high-order harmonics of the laser field.

B. Laser intensity dependence of the number of generated photons

Figures 8 and 9 present the number of photons at the third and fifth harmonics in Ne, Ar, Kr, and Xe (and also in He in Fig. 8) as a function of the laser intensity in a double logarithmic plot. The experimental uncertainty shown in this figure is much smaller than the one indicated in Figs. 4–6, because the uv photon energy has been kept constant. The curves closely follow straight lines with a slope of 3 ± 0.1 for the third harmonic (Fig.8) and a slope of 5 ± 0.2 for the fifth harmonic (Fig. 9) at low laser intensity. There is a saturation at high laser intensity, which takes place precisely at the saturation intensity for ionization (see Table I). This could indicate that ions do not contribute much to harmonic generation. The conversion efficiency saturates because the nonlinear medium responsible for the conversion is depleted. One may also think of breaking of phase-matching conditions due to the influence of free electrons in the medium.[15]

From these results, knowing the phase mismatches $\Delta k_3, \Delta k_5$ (see Table II) for the rare gases and therefore the phase-matching factor F_q for our experimental conditions [Fig.2(b)], we can deduce the (microscopic) nonlinear susceptibilities $\chi^{(3)}$ and $\chi^{(5)}$ [Eq. (7)]. These values are normalized to the third-order susceptibility of Xe, measured by Lehmeier *et al.*[29] using a Nd-glass laser (incident wavelength, 1.055 μm). They are indicated in Table II (in electrostatic units).

Figure 10 shows some laser-intensity dependences for

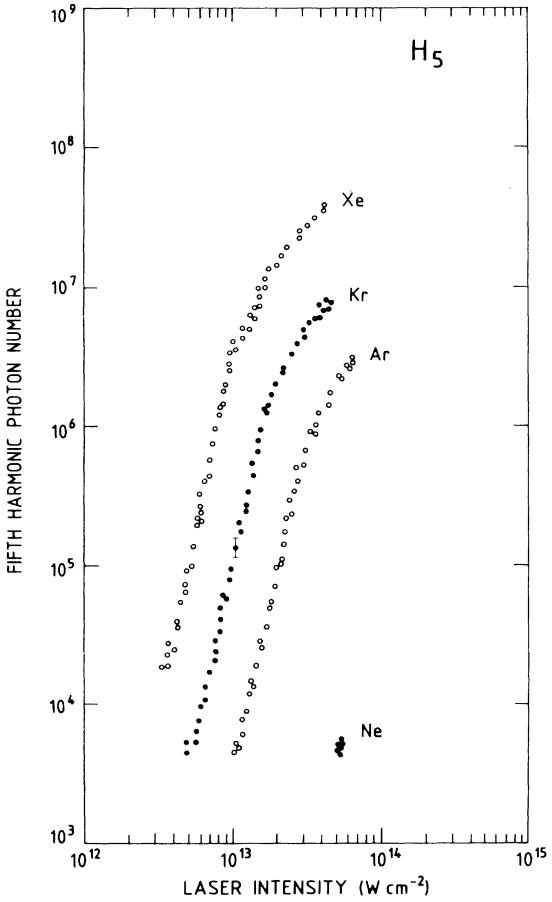

FIG. 9. Laser-intensity dependence of the number of photons at the fifth harmonic in Xe, Kr, Ar, and Ne, at a 15 Torr pressure.

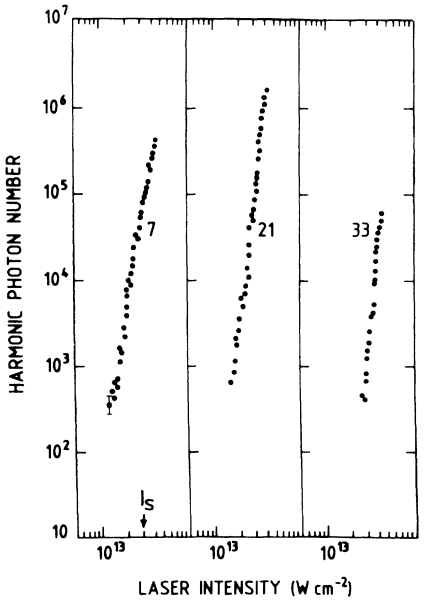

FIG. 10. Laser-intensity dependence of the number of photons at the 7th, 21st and 33rd harmonic in Ar, at 15 Torr.

higher-order harmonics, the 7th, 21st, and 33rd harmonics in argon. The experimental points for the seventh harmonic follow a straight line with slope 7.2±0.5, before the saturation intensity (I_s), varying slightly less rapidly above it. We think that seventh-harmonic generation can be understood within the framework of the perturbative theory developed in Sec. III. The seventh-order nonlinear susceptibility $\chi^{(7)}$, deduced from our results, is equal to 2×10^{-60} esu. In contrast, the 21st and 33rd harmonics deviate from the I^q law predicted by lowest-order perturbation theory. The slopes, determined by least-squares fitting over the whole intensity region (since there is no visible change around I_s), are, respectively, 8.2±0.5 and 12±1 for the 21st and 33rd harmonics.

C. Pressure dependence of the number of harmonic photons

Figure 11 presents the number of photons at the 17th harmonic produced in Kr, at 3×10^{13} W cm^{-2}, as a function of the gas pressure, in a log-log plot. The pressure is varied by displacing the nozzle of the gas jet, compared to the position of the laser focus, keeping the backing pressure constant. The experimental points in Fig. 11 are aligned upon a straight line, the slope of which is 1.8±0.1. Similar measurements for other harmonics and other gases lead to the same result, a straight line with a slope always slightly lower than 2, around 1.8. The deviation from the $\mathcal{N}^2$ power law [Eq. (7)] may be explained in terms of the variation of the *length* of the nonlinear medium as one increases the distance focus nozzle (the gas jet being slightly divergent). We have calculated the variation of the phase-matching factor F_q as a function of the length of the nonlinear medium, varying from 1 mm at 25 Torr to about 2.3 mm at 0.3 Torr (see Ref. 13). We compare in Fig. 11 the experimental data to the product $\mathcal{N}^2|F_q|^2$ (with $b=4$ mm; $\Delta k\approx0$ and L slowly varying with $\mathcal{N}$, as experimentally measured in Ref. 13) (solid

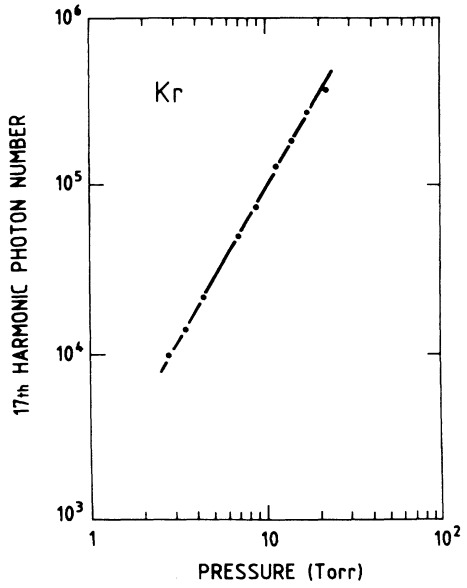

FIG. 11. Pressure dependence of the number of photons at the 17th harmonic in Kr, at 3×10^{13} W cm^{-2}.

line). This result is close to a $\mathcal{N}^{1.8}$ power law, in good agreement with the experimental data.

This result concerning the variation of the conversion efficiency with the gas pressure allows us to discuss the question of harmonic generation through *direct* or *indirect* processes (see Sec. III). If high-order harmonic generation were due to wave-mixing processes involving lower-order harmonic fields (what we call "indirect" processes), the conversion efficiency would vary much more rapidly with the pressure than $\mathcal{N}^2$. The systematic $\mathcal{N}^2$ (or $\mathcal{N}^{1.8}$) power law observed in the experiment probably means that high-order harmonic generation is a direct process, i.e., only involving the incident laser field.

D. Other light emission processes

In order to complete this description of vuv light emission processes in rare gases exposed to an intense laser field, we show in Fig. 12 typical experimental photon spectra obtained in Xe at 3×10^{13} W cm^{-2} and 15 Torr. Figure 12(a) is obtained with the electron multiplier over a 50–130-nm range; Figure 12(b) is obtained with a photomultiplier over a 110–160-nm range. The dominant features of these spectra are the harmonics of the laser field, from the 9th to the 21st in Fig. 12(a), and the 7th and 9th in Fig. 12(b). Their widths reflect the resolution of our detection system (≈ 8 Å); their relative amplitudes are meaningless, since no corrections have been made for including the spectral efficiency of the detection system. The other peaks shown in Fig. 12(a) are the second diffracted orders of the 21st, 19th, and 17th harmonics, not observed in Fig. 12(b) because of the different spectral range of the detectors employed. In addition, in Fig. 12(b), there are two lines corresponding to the transitions $6s\rightarrow 5p$ (147 nm) and $6s'\rightarrow 5p$ (129.5 nm) in neutral Xe. Over the whole spectrum extent (10–350 nm) in Ar, Kr, and Xe, we observe a small number of lines corresponding to transitions from excited states to the fundamental of the neutral atom and also of the singly charged ion. Much richer spectra have been observed by McPherson *et al.*[3] using a 248-nm laser at 10^{16} W cm^{-2}, for more ionized species (Xe^{6+}, Xe^{7+}). Finally, Fig. 12(a) also shows a significant *continuous background.* This broad continuum emission is rather intense in Xe, insignificant in Kr, and practically nonexistent in Ar at the same laser intensity (3×10^{13} W cm^{-2}).

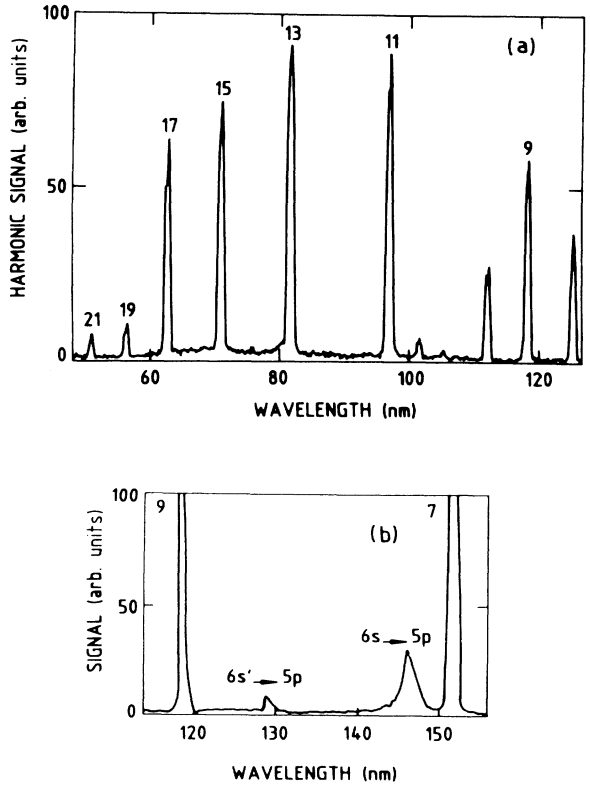

FIG. 12. Photon spectra obtained at 1064 nm, 3×10^{13} W cm^{-2}, 15 Torr; (a) from 50 to 130 nm using the electron multiplier; (b) from 110 to 160 nm using the EMI photomultiplier.

In order to gain more information on these light emissions processes, we have performed time-resolved measurements at particular wavelengths and intensities. Figure 13 shows, for example, a record obtained with a 100-MHz-bandwidth Lecroy oscilloscope at 147 nm, corresponding to the $6s\rightarrow 5p$ transition in Xe. The width of the broad peak in Fig. 13 is equal to 3 μsec. This slow emission, which disappears at lower intensity, is probably the last step of a series of radiative deexcitation processes, originating from plasma recombination processes. The sharp peak in Fig. 13 is characteristic of the continuum emission since it can be observed over the whole uv spectrum range, whereas, in contrast, the broad peak in Fig. 13 appears only at 147 nm. Its width, of the order of 10 nsec, is that of the detection system. The origin of this continuum emission is not yet fully understood. More systematic studies (e.g., intensity or pressure dependences) are needed for identifying the physical effect responsible for this light emission. It does not seem to be a molecular type of recombination continuum since it is a fast process of duration smaller than 10 nsec and probably of the same time scale as the laser pulse duration. It could be a parametric type of process, such as the emission induced by self-phase modulation[30] (of the incident or harmonic fields) or stimulated Raman scattering effects.

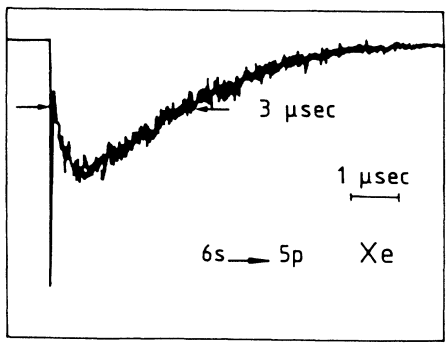

FIG. 13. Time-resolved measurement performed at 3×10^{13} W cm^{-2}, 15 Torr and 147 nm.

V. SUMMARY AND CONCLUSION

The study of the interaction of a dense medium of rare-gas atoms with a strong laser field has led to rather unexpected but exciting results. In the ultraviolet region, apart from a small number of emission lines which we attribute to plasma recombination processes and also a broad continuum emission, we essentially observe the harmonics of the incident laser field, up to very high-order. As shown in multiphoton ionization experiments, there is a strong coupling between a rare-gas and an intense infrared radiation field, which enables the observation of extremely high-order nonlinear processes. In our opinion, there is certainly an analogy between above-threshold ionization and harmonic generation when the energy of the generated photon exceeds the ionization energy.[31,32] In the first process, the absorption of a large number of photons leads to the ionization of the atom with ejection on an energetic electron; in the latter case, the absorbed energy is transferred to a different mode of the photon field. These two competing phenomena originate from the same interaction but lead to different final states (ion+electron in the first case; atom+harmonic photon in the second case). In particular, since the use of femtosecond laser pulses has recently shown the influence of resonant processes in multiphoton ionization,[33] one could imagine that, in the same way, resonances could play an important role in high-order harmonic generation. An important theoretical effort is presently under way for understanding harmonic generation from an atom exposed to an intense laser field.[32,34–36]

However, there is also a collective aspect to harmonic generation, involving the response of the whole medium to the external field. The interplay between microscopic and macroscopic properties of a nonlinear medium in an intense field makes the interpretation of the experimental results rather complex. In the present work, we have tried to disentangle both aspects, by characterizing as well as possible the phase-matching conditions in our experiment, at least in a weak-field approximation.

The key point of our experimental results is the following: the average distribution of the harmonics first decreases rather steeply from the third to the seventh harmonic, then presents a kind of plateau, with no change in the harmonic-field amplitude as the energy of the harmonic photon crosses the ionization threshold, and finally decreases again rather steeply. The first harmonics behave (for the intensity as well as the pressure dependence) according to theoretical predictions derived from lowest-order perturbation theory, with proper inclusion of phase-matching conditions. The anomaly in the Ar harmonic distribution for the 13th harmonic may be explained by the influence of discrete excited states. However, neither the extended plateau (from the 9th harmonic to the 21st harmonic in Ar), nor the cutoff at high order can be explained by the traditional theory of nonlinear optics in weak field (nor by any phase-matching arguments). The intensity dependence of the high-order harmonics suggests a behavior going beyond lowest-order perturbation theory.

We have tried to estimate the number of harmonic photons produced in absolute value. The conversion efficiency, defined by $\xi_q = qN_q/N_1$ (N_q denoting the number of generated photons at each laser shot), is of the order of 10^{-8} and 10^{-10} for third-harmonic generation in Xe and Ar, respectively, at 10^{13} W cm^{-2}, 10^{-11} for the 25th harmonic (in the plateau region) and 10^{-13} for the 33rd harmonic in Ar, at 15 Torr and 3×10^{13} W cm^{-2}. The spectral brightness of a vuv light source is often expressed in photons/(Å s mrad^2) (Ref. 37). Assuming a Gaussian distribution for the laser field and its harmonics, we have $\Delta\lambda_q = 0.2\sqrt{q}$ Å, $\tau_q = 36/\sqrt{q}$ psec, and $\theta_q = 13/\sqrt{q}$ mrad. The brightness of our vuv light source, for example, in the region of the plateau in Xe, is then equal to 10^{17} photons/(Å s mrad^2). This brightness (unfortunately with a very low repetition rate limited to 10 Hz and no tunability) is considerably higher than the brightness of the Anneau de Collisions d'Orsay (ACO) synchrotron radiation source,[37] of the order of 10^{12} photons/(Å s mrad^2) (with, however, a much higher repetition rate, about 20 MHz). Multiple-harmonic conversion in rare gases gives vuv radiation of substantially higher spectral brightness per pulse than other radiation sources in this spectral region and therefore could be used in vuv spectroscopy.

ACKNOWLEDGMENTS

We would like to thank Dr. C. Manus for many stimulating discussions, and A. Sanchez and D. Fondant for their technical assistance in the experiments.

[1]See articles in *Multiphoton Processes*, Proceedings of the Fourth International Conference on Multiphoton Processes, Joint Institute for Laboratory Astrophysics, Boulder, 1987, edited by S. J. Smith and P. L. Knight (Cambridge University Press, Cambridge, England, 1988).

[2]M. Ferray, A. L'Huillier, X. F. Li, L. A. Lompré, G. Mainfray, and C. Manus, J. Phys. B **21**, L31 (1988).

[3]A. McPherson, G. Gibson, H. Jara, U. Johann, T. S. Luk, I. McIntyre, K. Boyer, and C. K. Rhodes, J. Opt. Soc. Am. B **4**, 595 (1987).

[4]M. G. Groseva, D. I. Metchkov, V. M. Mitev, L. I. Pavlov and K. V. Stamenov, Opt. Commun. **23**, 77 (1977).

[5]J. Wildenauer, J. Appl. Phys. **62**, 41 (1988).

[6]J. Reintjes, C. Y. She, and R. Reckardt, IEEE J. Quantum Electron. **QE-14**, 581 (1978).

[7]J. Reintjes, L. L. Tankersley, and R. Christensen, Opt. Commun. **39**, 334 (1981).

[8]J. Bokor, P. H. Bucksbaum, and R. R. Freeman, Opt. Lett. **8**, 217 (1983).

[9]J. Reintjes, C. Y. She, R. C. Eckardt, N. E. Karangelen, R. A. Andrews, and R. C. Elton, Appl. Phys. Lett. **30**, 480 (1977).

[10]H. Puell, K. Spanner, W. Falkenstein, W. Kaiser, and C. R. Vidal, Phys. Rev. A **14**, 2240 (1976).

[11]R. Rosman, G. Gibson, K. Boyer, H. Jara, T. S. Luk, I. A. McIntyre, A. McPherson, J. C. Solem, and C. K. Rhodes, J. Opt. Soc. Am. B **5**, 1237 (1988).

[12]A. L'Huillier, L. A. Lompré, G. Mainfray, and C. Manus, J. Phys. B **16**, 1363 (1983). The saturation intensities for He and Ne had been overestimated by a factor of 2.
[13]L. A. Lompré, M. Ferray, A.L'Huillier, X. F. Li, and G. Mainfray, J. Appl. Phys. **63**, 1791 (1988).
[14]J. A. R. Samson, *Techniques of Vacuum Ultraviolet Spectroscopy* (Wiley, New York, 1967), p. 229.
[15]J. F. Reintjes, *Nonlinear Optical Parametric Processes in Liquids and Gases* (Academic, New York, 1984).
[16]See also N. Bloembergen, *Nonlinear Optics* (Benjamin, New York, 1965); D. C. Hanna, M. A. Yuratich, and D. Cotter, *Nonlinear Optics of Free Atoms and Molecules* (Springer-Verlag, Berlin, 1979).
[17]I. V. Tomov and M. C. Richardson, IEEE J. Quantum Electron. **QE-12**, 521 (1976).
[18]D. A. Kleiman, A. Ashkin, and G. D. Boyd, Phys. Rev. **145**, 338 (1966).
[19]J. F. Ward and G. H. C. New, Phys. Rev. A **185**, 57 (1969).
[20]G. C. Bjorklund, IEEE J. Quantum Electron. **QE-11**, 287 (1975).
[21]A. Lago, G. Hilber, and R. Wallenstein, Phys. Rev. A **36**, 3827 (1987).
[22]P. J. Leonard, At. Data Nucl. Data Tables **14**, 21 (1974).
[23]R. B. Miles and S. E. Harris, IEEE J. Quantum Electron. **QE-9**, 470 (1973); S. E. Harris, Phys. Rev. Lett. **31**, 341 (1973).
[24]L. J. Zych and J. F. Young, IEEE J. Quantum Electron **QE-14**, 147 (1978).
[25]H. Scheingraber, H. Puell, and C. R. Vidal, Phys. Rev. A **18**, 2585 (1978).
[26]A. L'Huillier, L. A. Lompré, M. Ferray, X. F. Li, G. Mainfray, and C. Manus, Europhys. Lett. **5**, 601 (1988).
[27]R. L. Carman, C. K. Rhodes, and R. F. Benjamin, Phys. Rev. A **24**, 2649 (1981).
[28]M. B. Isichenko and V. V. Yan'kov, Zh. Eksp. Teor. Fiz. **87**, 1914 (1984) [Sov. Phys.—JETP **60**, 1101 (1984)].
[29]H. J. Lehmeier, W. Leupacher, and A. Penzkofer, Opt. Commun. **56**, 67 (1985).
[30]P. B. Corkum, C. Rolland, and T. Srivanasan-Rao, Phys. Rev. Lett. **57**, 2268 (1986).
[31]B. W. Shore and P. L. Knight, J. Phys. B **20**, L413 (1987).
[32]J. H. Eberly, Q. Su, and J. Javanainen, Phys. Rev. Lett. **62**, 881 (1989).
[33]R. R. Freeman, P. H. Bucksbaum, H. Milchberg, S. Darach, D. Schumacher, and M. E. Geusic, Phys. Rev. Lett. **59**, 1092 (1987).
[34]K. C. Kulander and B. W. Shore, Phys. Rev. Lett. **62**, 524 (1989).
[35]R. M. Potvliege and R. Shakeshaft (private communication).
[36]There are also perturbative calculations of very high-order nonlinear susceptibilities in H; see, e.g., Y. Gontier and M. Trahin IEEE J. Quantum Electron. **QE-18**, 1137 (1982); B. Gao and A. F. Starace, Phys. Rev. A **39**, 4550 (1989); L. Pan, K. T. Taylor, and C. W. Clark (private communication); R. M. Potvliege, and R. Shakeshaft, Z. Phys. D, **11**, 93 (1989).
[37]J. M. Bizeau, thèse de doctorat, Paris, 1987.